ELSEVIER

Available online at www.sciencedirect.com
SCIENCE DIRECT®

Thin Solid Films 425 (2003) 145–149

thin solid films

www.elsevier.com/locate/tsf

Residual stress induced atomic scale buckling of diamond carbon coatings on silicon substrate

K. Mylvaganam, L.C. Zhang*

School of Aerospace, Mechanical and Mechatronic Engineering, The University of Sydney, Sydney, NSW 2006, Australia

Received 23 April 2002; received in revised form 22 October 2002; accepted 10 December 2002

Abstract

This paper investigates the atomic scale buckling of diamond carbon coatings on silicon substrate caused by residual stresses in two orthogonal directions. It was found that different buckling patterns occurred when the ratio of the residual stresses in the two directions were changed. The size of wrinkles increased on going from uniaxial to biaxial compression of the residual stress fields. A telephone-cord like buckling mode took place when the residual stresses were bi-axially equal.
© 2002 Elsevier Science B.V. All rights reserved.

Keywords: Buckling; Coatings; Computer simulation; Stress

1. Introduction

Coatings have industrial applications in many engineering components. Both soft and hard coatings can inhibit adhesion between the substrate and the counter face resulting in decreased wear. They may also make surface defects less harmful by moving crack initiation sites from the surface down to subsurface regions, thus improving the performance of the substrate.

Carbon coatings on silicon substrates are very common. Various techniques such as chemical vapour deposition (CVD) and pulse laser deposition are being used to deposit carbon on to silicon [1]. Depending on the technique and conditions, either amorphous carbon films or diamond-like carbon films can be produced, of which the latter exhibit high density, extreme hardness, high thermal conductivity, chemical inertness, and infrared transparency. However, the films often suffer from adhesion problems—partially or totally delaminated at the interface or in the substrate due to high compressive stresses [2–13]. For example, Freller et al. [3] showed that when the compressive stress in a film exceeds the ultimate tensile strength of the substrate, failure occurs in the substrate. Zehnder et al. [4] reported that a film deposited at 20 °C showed no evidence of failure in the bulk, but delaminated at the interface, all over the sample. On the other hand, a film grown at 500 °C would adhere very well to the silicon substrate but would delaminate when its thickness exceeds 600 nm. Som et al. [5] studied the delamination of CVD diamond films deposited on silicon and estimated that the biaxial compressive stress to initiate the film buckling was 1.19 GPa.

Buckling/delamination of a coating is unwanted in industrial applications. Thus a fundamental understanding of the stress relief patterns or buckling modes and the stress levels at which buckling occurs is necessary. Some very interesting buckling patterns such as telephone-cord, sinusoidal wave, sinusoidal shape with extra branches and a strings-of-beads pattern have been reported in Refs. [7,9,10]. Gioia and Ortiz [2] have compiled most of these patterns in their paper on delamination of compressed thin films. However, the studies to date have been mainly using experimental techniques and continuum mechanics. Although Pailthorpe et al. [14], McKenzie et al. [15], and Rosenblum et al. [16] used atomistic simulation in their studies on coating they concentrated mainly on the energy diffusion, the structure of films and the mismatch-induced residual thermal stresses in film/substrate systems.

The present study uses molecular dynamics simulation to investigate the atomic scale buckling modes of diamond carbon films deposited on silicon.

*Corresponding author. Tel.: +61-2-9351-2835; fax: +61-2-9351-7060.
E-mail address: zhang@mech.eng.usyd.edu.au (L.C. Zhang).

0040-6090/03/$ - see front matter © 2002 Elsevier Science B.V. All rights reserved.
PII: S0040-6090(02)01287-7

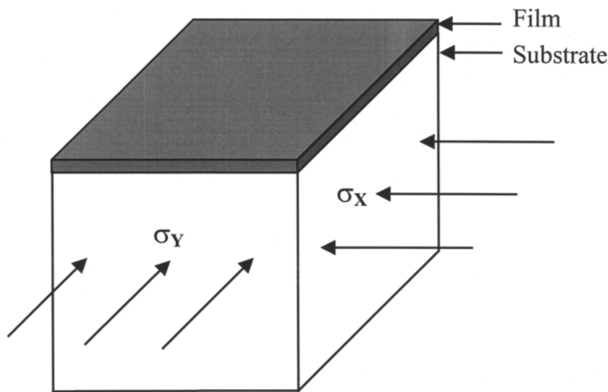

Fig. 1. The simulation model.

2. Simulation method

The buckling of a thin film is caused by local compressive stresses on the film, introduced by the coating process. Thornton [17] pictured this process as follows: first the incident atoms transfer kinetic energy to the substrate and become loosely bonded 'ad atoms'. They then diffuse over the surface exchanging energy with the substrate until they are either desorbed or trapped at low energy sites of the substrate. Thus the initial kinetic energy transfer to the substrate can induce a tensile stress on the substrate. When the atoms diffuse over the surface, a compressive stress can be induced back to the coated atoms. In the present molecular dynamics simulation, for convenience but still capturing the nature of the residual stress generation, we apply the tensile stresses on the substrate before placing the coating and then release the stress with the coating on, so that the film will undergo compressions as experienced in experiment.

Table 1
Parameters for the Morse potential $V(r_{ij})=D[e^{-2\alpha(r_{ij}-r_0)}-2e^{-\alpha(r_{ij}-r_0)}]$

Parameter	Si–C
α (Å^{-1})	4.6417
D (kcal mol^{-1})	100.32
r_0 (Å)	1.9475

We focus on the deformation of a diamond carbon coating on silicon under various stress levels with different ratios of compressive stresses in two perpendicular directions, X and Y, as shown in Fig. 1. A piece of diamond cubic silicon (1 0 0) with the control volume of $10.3\times10.3\times3.8$ nm^3 (i.e. 19 unit cells$\times$19 unit cells$\times$7 unit cells), containing 21 516 atoms, was used as a substrate. The outermost layer of the substrate atoms with the exception of the top (1 0 0) surface was

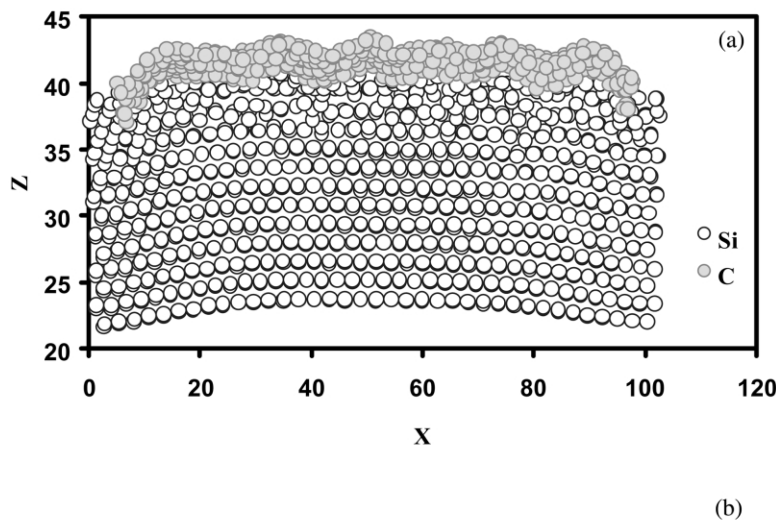

Fig. 2. (a) A cross-section of portion of the film and substrate. (b) Sinusoidal buckling pattern of the top layer of the film in X-direction, after releasing the uniaxial stress ($\sigma_y/\sigma_x=0$).

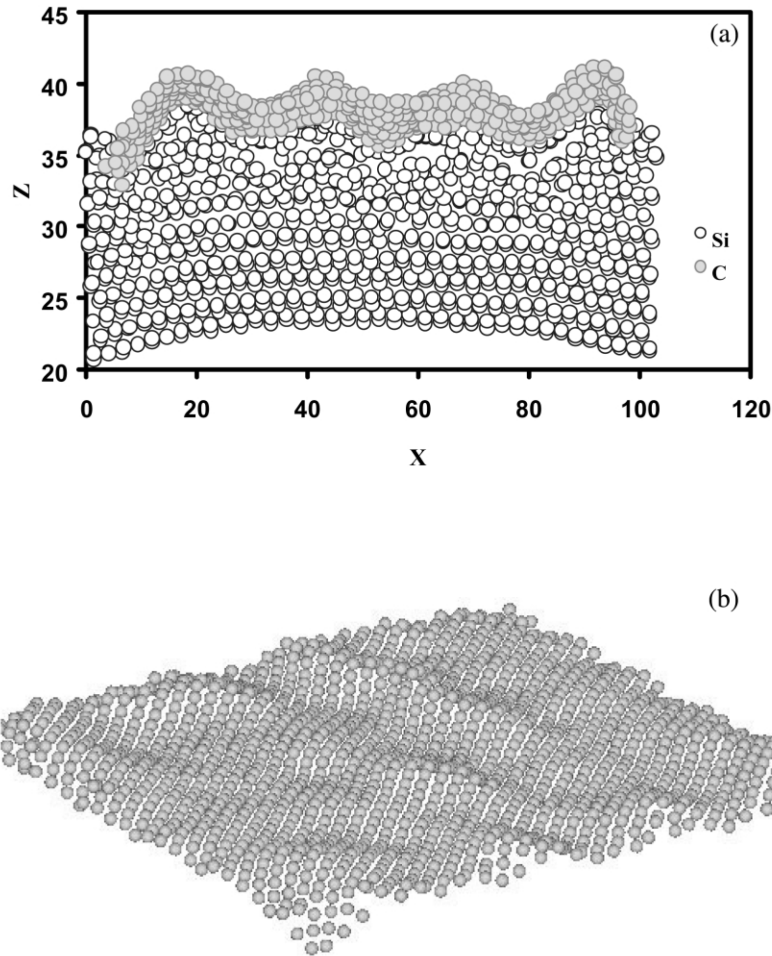

Fig. 3. (a) A cross-section of portion of the film and substrate. (b) Wavy buckling pattern of the top layer of the film, after releasing the biaxial stresses ($\sigma_y/\sigma_x \approx 0.5$).

thermo-stated to 300 K. The tensile stresses were applied by forced atomic displacements at the boundary of the control volume in the following distinct ways to uncover the effect of stress variation in the film plane: (i) uniaxially (along the *X*-direction), i.e. the stress externally applied in *Y*-direction would be zero and hence the stress ratio is $\sigma_y/\sigma_x=0$, (ii) bi-axially with less displacement along *Y*-direction to give the stress ratio of $\sigma_y/\sigma_x \approx 0.5$, and (iii) bi-axially with equal displacements along both *X*- and *Y*-directions to give the stress ratio of $\sigma_y/\sigma_x \approx 1$. Three atomic layers of diamond coating with dimensions $9.987 \times 9.987 \times 0.1783$ nm^3, having 4817 atoms was placed on the stressed substrate. The coating and substrate were relaxed together for 5 Ps and then the stresses on the substrate were released gradually.

A three-body Tersoff potential [18,19], which has been used in many successful MD simulation studies [20–24], was used for Si–Si and C–C interactions. A two-body Morse potential was used for C–Si interactions with the parameters shown in Table 1. This potential has been proved to be reliable in describing C–Si, C–Cu and C–Al interactions [23–28]. Since the purpose of this study is to explore the deformation patterns of the film, to facilitate the observation of the buckling deformation, we apply sufficiently large stresses, much higher than the critical buckling stress measured in relevant experiments [5,7], provided that they are within the elastic limit of silicon.

3. Results and discussion

3.1. Observations

3.1.1. Substrate under uniaxial stress ($\sigma_y/\sigma_x=0$)

When subjected to a uniaxial stress σ_x, we find that the substrate of mono-crystalline silicon deforms plastically at a Cauchy stress (also known as true stress and defined as force/current area) of 16.0 GPa. Hence in the present study the coating was placed on the substrate pre-tensioned to 12.5 GPa at which the silicon substrate still deforms elastically. Fig. 2a shows a cross-section

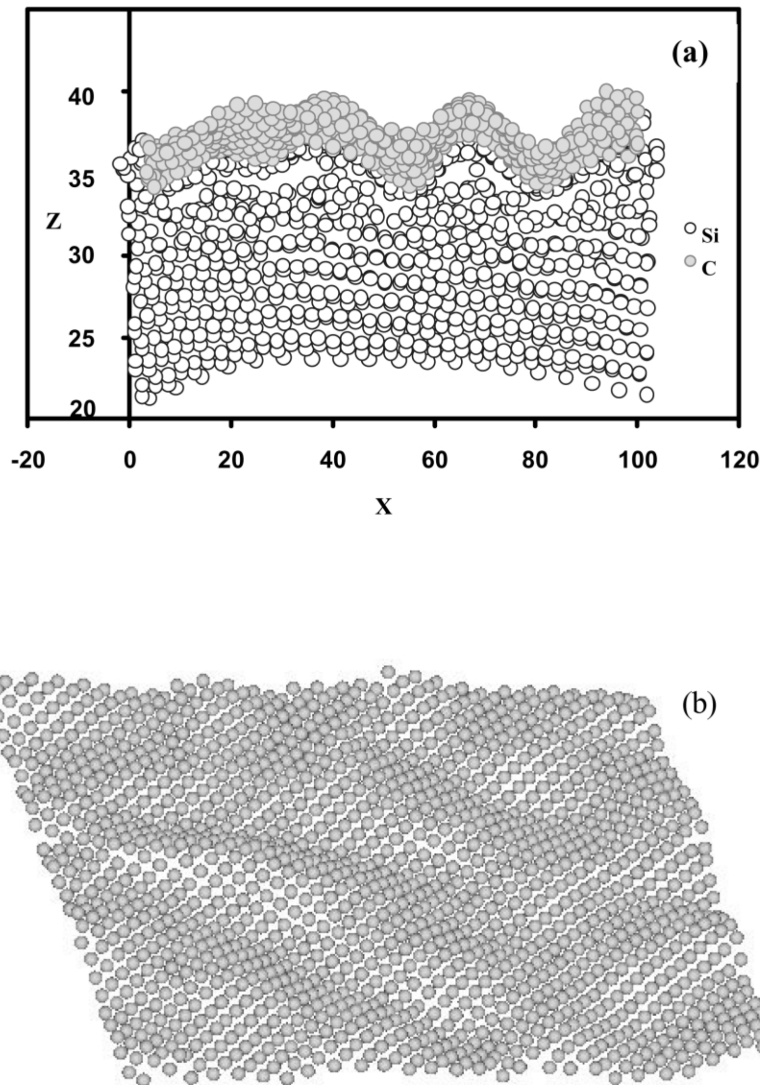

Fig. 4. (a) A cross-section of portion of the film and substrate. (b) Telephone-cord like buckling pattern of the top layer of the film, after releasing the biaxial stresses ($\sigma_y/\sigma_x \approx 1$).

of part of the substrate and film after releasing the stress on the substrate. The film buckled and slightly delaminated in some places at the film-substrate interface. The top layer of the film viewed from the top, at a tilted angle, is shown in Fig. 2b. This presents an interesting buckling pattern with sinusoidal wrinkles mainly in *X*-direction along which the stress applied.

3.1.2. Substrate under bi-axially unequal stresses ($\sigma_y/\sigma_x \approx 0.5$)

In this case the substance deforms plastically at a Cauchy stress of 18.32 GPa in the *X*-direction and 9.72 GPa in the *Y*-direction. Coating was placed on the substrate having the same strain along *X* as in case (i) with $\sigma_x = 15.10$ GPa and $\sigma_y = 8.86$ GPa which were well below the above critical stress values. Fig. 3a shows a cross-section of part of the substrate and film after releasing the stress on the substrate. The film buckled and delaminated, but the delamination occurred only at certain places at the interface. The deformation in the top most layer of the film is shown in Fig. 3b. It is clear that the size of the wrinkles is bigger than that of case (i) but the buckling mode in the present case is no longer uni-axially sinusoidal. The application of σ_y created the wavy in *Y*-direction as well.

3.1.3. Substrate under bi-axially equal stresses ($\sigma_y/\sigma_x \approx 1$)

Now the substrate starts to deform plastically at a Cauchy stress of 13.8 GPa in both *X*- and *Y*-directions. The coating was placed on the substrate having the same strain along *X* as in case (i) with both σ_x and $\sigma_y = 13.4$ GPa which were below the above critical values. Again on releasing the stress the film buckled

and delaminated. A cross-section of part of the film and substrate is shown in Fig. 4a and the top most layer of the film is shown in Fig. 4b. Now it is interesting to note that the size of the wrinkles becomes larger than those in both cases (Sections 3.1.1 and 3.1.2) and the overall buckling pattern approaches a telephone-cord like structure as observed in many experiments.

3.2. Discussion

In all the three cases, although the delamination occurs at the interface, the film tends to attract a layer of Si atoms. This is because both the C–C interaction (348 $kJ\,mol^{-1}$) and the C–Si interaction (285 $kJ\,mol^{-1}$) are greater than the Si–Si interaction (176 $kJ\,mol^{-1}$) [29] so that the Si atoms are attracted towards the C-film when the film possesses a considerable bending rigidity. The results show that within each case, the buckling mode and the size of the wrinkles did not change significantly, but the pattern became more pronounced, on completely releasing the stress. On the other hand, the buckling mode did vary with the σ_y/σ_x ratio, from mainly a sinusoidal mode with $\sigma_y/\sigma_x = 0$ to a telephone-cord like structure when $\sigma_y/\sigma_x \approx 1$.

4. Conclusions

Thin film buckling does occur on the atomic scale when the compressive stresses in a film are sufficiently high. The buckling mode varies with σ_y/σ_x, indicating that the stress ratio is an important factor that influences the nature of the buckling patterns. It is interesting to note that the pattern of atomic scale buckling of a thin film is similar to that observed in micro-scale experiments.

Acknowledgments

The authors would like to thank the Australian Research Council for the continuous financial support, and the valuable discussion with Dr Y.G. Shen at Department of MEEM, City University of Hong Kong.

References

[1] M. Ohring, Materials Science of Thin Films, Academic Press, San Diego, 2002.
[2] G. Gioia, M. Ortiz, Adv. Appl. Mech. 33 (1997) 120.
[3] H. Freller, A. Hempel, J. Lilge, H.P. Lorenz, Diamond Relat. Mater. 1 (1992) 563.
[4] T. Zehnder, J. Balmer, W. Luthy, H.P. Weber, Thin Solid Films 263 (1995) 198.
[5] T. Som, S. Bhargava, M. Malhotra, H.D. Bist, V.N. Kulkarni, S. Kumar, Appl. Phys. Lett. 72 (1998) 3014.
[6] X.L. Peng, T.W. Clyne, Thin Solid Films 312 (1998) 207.
[7] S.B. Iyer, K.S. Harshavardhan, V. Kumar, Thin Solid Films 256 (1995) 94.
[8] J.W. Ager III, M.D. Drory, Phys. Rev. B 48 (1993) 2601.
[9] G. Gille, B. Rau, Thin Solid Films 120 (1984) 109.
[10] D. Nir, Thin Solid Films 112 (1984) 41.
[11] B. Audoly, Phys. Rev. Lett. 83 (1999) 4124.
[12] K.M. Crosby, R.M. Bradley, Phys. Rev. E 59 (1999) R2542.
[13] P. Peyla, Phys. Rev. E 62 (2000) 1501.
[14] B.A. Pailthorpe, D. Mitchell, N.S. Bordes, Thin Solid Films 332 (1998) 109.
[15] D.R. McKenzie, D. Muller, B.A. Pailthorpe, Phys. Rev. Lett. 67 (1991) 773.
[16] I. Rosenblum, J. Adler, S. Brandon, A. Hoffman, Phys. Rev. B 62 (2000) 2920.
[17] J.A. Thornton, Annu. Rev. Mater. Sci. 7 (1977) 239.
[18] J. Tersoff, Phys. Rev. B 39 (1989) 5566.
[19] J. Tersoff, Phys. Rev. Lett. 56 (1986) 632.
[20] J. Belak, D.B. Boercker, I.F. Stowers, Mater. Res. Soc. Bull. 18 (1993) 55.
[21] T. Inamura, S. Shimada, N. Takezawa, N. Ikawa, Ann. CIRP 48 (1999) 81.
[22] S. Shimada, N. Ikawa, T. Inamura, H. Ohmori, T. Sata, Ann. CIRP 44 (1995) 523.
[23] R. Komanduri, N. Chandrasekaran, L.M. Raff, Philos. Mag. B 81 (2001) 1989.
[24] L.C. Zhang, H. Tanaka, JSME Int. J. Ser. A 42 (1999) 546.
[25] W.C.D. Cheong, L.C. Zhang, Nanotechnology 11 (2000) 1.
[26] L.C. Zhang, H. Tanaka, Tribol. Int. 31 (1998) 425.
[27] R. Komanduri, N. Chandrasekaran, L.M. Raff, Wear 242 (2000) 60.
[28] R. Komanduri, N. Chandrasekaran, L.M. Raff, Wear 240 (2000) 113.
[29] D.R. Lide, CRC Handbook of Chemistry and Physics, Chemical Rubber Company Press, Boca Raton, FL, 2000–2001.